MAGNETIC RESONANCE IN CHEMISTRY, VOL. 35, 757–764 (1997)

Cross-Polarization Dynamics and Proton Dipolar Local Field Measurements in Some Organic Compounds

Pierre Reinheimer,[1] Jérôme Hirschinger,[1]* Patrick Gilard[2] and Noël Goetz[2]
[1] Institut de Chimie, UMR 50 CNRS, Bruker Spectrospin, Université Louis Pasteur, BP 296, 67008 Strasbourg Cedex, France
[2] L'Oréal, Laboratoires de Recherche Avancée, 1 avenue E. Schueller, 93600 Aulnay sous Bois, France

Hartmann–Hahn inversion–recovery cross-polarization magic-angle spinning experiments were performed for all types of protonated carbons (CH_n with $n = 1$, 2 and 3). The resulting non-exponential decays were analyzed using both a simple memory function approach and density matrix calculations. Although the memory function approach provides a useful analytical description of the cross-polarization dynamics, the density matrix method is required to account better for the details of the spin dynamics. ^{13}C-detected dipolar local fields of protons were measured using the wideline separation experiment. It was observed that the resulting local free induction decays may be quantitatively described by their local second moment. Moreover, the local spin diffusion process controlling the second stage of the cross-polarization dynamics is directly related to the strength of the local dipolar field of protons.

Magn. Reson. Chem. **35**, 757–764 (1997) No. of Figures: 7 No. of Tables: 0 No. of References: 52

Keywords: NMR; cross-polarization; magic-angle spinning; local field spectroscopy; spin diffusion

Received 6 March 1997; revised 3 June 1997; accepted 10 June 1997

INTRODUCTION

For more than two decades, Hartmann–Hahn (HH) cross-polarization (CP) has been undoubtedly the most widely used technique for enhancing the nuclear magnetization of a rare spin system in magic-angle spinning (MAS) NMR spectroscopy.[1–3] When the fluctuations of the local field governing the spin diffusion process are faster than the exchange of magnetization between the two spin systems (fast-correlation assumption), CP proceeds exponentially as cross-relaxation.[2,4–6] In this case, the abundant spin system behaves as a thermal bath and the spin temperature concept can be applied. On the other hand, the presence of strong heteronuclear interactions, as in the case of protonated carbons, leads to coherent energy transfer.[2,6–8] The resulting two-stage character of the polarization transfer for rigid or semi-rigid CH_n groups ($n = 1$, 2) has been previously observed and analyzed in both static and rotating samples.[9–16] Moreover, several CP/MAS pulse sequences have been developed to simplify spectra of complex molecules. Opella and Frey[17] introduced the delayed decoupling or 'dipolar dephasing' (DD) sequence designed to differentiate between resonances for protonated and non-protonated carbons due to their different heteronuclear dipolar dephasing rates in the laboratory frame. An alternative approach using CP dynamics resulted in several spectral-editing methods[18–26] based on the inversion–recovery cross-polarization (IRCP) pulse sequence originally introduced by Melchior.[27] Although both the DD and IRCP techniques are very dependent on the C–H dipolar coupling network, discrimination between CH and CH_2 groups in rigid solids is not straightforward.[23–26] Moreover, it has been shown recently, that CP also permits the indirect observation of the local field[28–34] and also the spin diffusion process[35,36] of the abundant I nuclei via spy detection by the rare S nuclei in the case of strongly coupled I and S spins (e.g. CH and CH_2 groups). Indeed, in this case, the S spins can be polarized very rapidly.

In this paper, we examine the cross-polarization dynamics for all types of protonated carbons. The experimental results are analyzed both by a simple memory function approach and by a density matrix method. On the other hand, local dipolar fields of protons are measured and related to the spin diffusion process which is known to control the second stage of the cross-polarization dynamics.[7,9,13,14]

THEORETICAL CONSIDERATIONS

The determination of the CP dynamics from first principles for a static single crystal of sufficiently simple structure already represents a formidable task.[5] Such an exact calculation becomes practically impossible for powders of complex structure in the presence of MAS. Appropriate mathematical approximations must then

* Correspondence to: J. Hirschinger at Institut de Chimie, UMR 50 CNRS, Bruker Spectrospin, Université Louis Pasteur, BP 296, 67008 Strasbourg Cedex, France

 CCC 0749–1581/97/110757–08 $17.50

be made. Two different approaches are used here: the first is a simple analytical method based on a spin correlation function, the memory function, and the other uses the density matrix and involves the numerical integration of the quantum mechanical master equation.

Memory function approach

We consider the magnetizations of a particular S spin (^{13}C) and its n directly attached I spins (^{1}H). Assuming that the heteronuclear I–S interactions are larger than any I–I couplings, the deviations of the magnetization of the S spin and of the n attached spins I from their equilibrium values $m_S(t) = M_S(t) - M_S(\infty)$ and $m_I(t) = M_I(t) - M_I(\infty)$, respectively, can be described by the following differential equation:[2,6]

$$\frac{\mathrm{d}}{\mathrm{d}t} m_S(t) = -\frac{\mathrm{d}}{\mathrm{d}t} m_I(t) = -\int_0^t K(t-\tau) m_S(\tau)\,\mathrm{d}\tau + \int_0^t K(t-\tau)\frac{m_I(\tau)}{n}\,\mathrm{d}\tau \tag{1}$$

where an ansatz for the memory function (autocorrelation function) $K(t)$ in a powder MAS experiment is given by[37]

$$K(t) = \frac{M_2^{IS}}{2}\left[\frac{2}{3}\cos(\omega_r t) + \frac{1}{3}\cos(2\omega_r t)\right]\exp\left(-\frac{t}{\tau_c}\right) \tag{2}$$

where M_2^{IS} is the second moment of the I–S dipolar couplings, $v_r = \omega_r/2\pi$ is the spinning frequency and τ_c is the correlation time of $K(t)$. The derivation of Eqn (1) from Mori's Langevin equation is given in Appendix B of the paper by Cheung and Yaris.[6] The choice of an exponential decay for $K(t)$ is a matter of mathematical convenience so that we can calculate the time integrals in Eqn (1) analytically. Substituting Eqn (2) into Eqn (1) and applying the Anderson–Weiss approximation,[2,37,38] one finds the following analytical solution for $u(t) = m_S(t) - m_I(t)/n$:

$$u(t) = u(0)\exp\left\{\frac{1+n}{2n} M_2^{IS}\left[\frac{2}{3} f(\Gamma, \omega_r, t) + \frac{1}{3} f(\Gamma, 2\omega_r, t)\right]\right\} = u(0)\exp\{\cdots\} \tag{3}$$

where

$$f(\Gamma, \omega_r, t) = \frac{1}{\Gamma^2 + \omega_r^2} \times \left\{\frac{[(\omega_r^2 - \Gamma^2)\cos\omega_r t + 2\Gamma\omega_r \sin\omega_r t]\exp(-\Gamma t)}{\Gamma^2 + \omega_r^2} - \Gamma t\right\} + \frac{\Gamma^2 - \omega_r^2}{(\Gamma^2 + \omega_r^2)^2}$$

and $\Gamma = 1/\tau_c$.

If, in addition, the CH_n subsystem is interacting with the remaining protons by the spin diffusion process characterized by a longer time τ_D, we may further write, neglecting spin–lattice relaxation ($T_{1\rho}$)[6]

$$m_I(t) + m_S(t) = [m_I(0) + m_S(0)]\exp\left(-\frac{t}{\tau_D}\right) \tag{4}$$

Equation (3) and (4) then lead to the following relationship:

$$m_S(t) = \frac{m_I(0) + m_S(0)}{n+1}\exp\left(-\frac{t}{\tau_D}\right) + \frac{nm_S(0) - m_I(0)}{n+1}\exp\{\cdots\} \tag{5}$$

Introducing the initial and final magnetizations into Eqn (5) for the IRCP experiment, we obtain finally the relevant analytical expression of the carbon magnetization:

$$S(t) = \frac{M_S(t)}{M_{0S}} = -1 + \frac{2}{n+1}\exp\left(-\frac{t}{\tau_D}\right) + \frac{2n}{n+1}\exp\{\cdots\} \tag{6}$$

where M_{0S} is the equilibrium magnetization of the rare S spins after the initial CP period of the IRCP sequence. Equation (6) demonstrates that, in the absence of spin diffusion ($\tau_D \to \infty$), i.e. for an isolated CH_n group, $S(t)$ would reach an equilibrium value of $(1-n)/(n+1)$. Indeed, for a static sample when $M_2^{IS} \gg \Gamma^2$, Eqn. (6) reduces to the simple expression

$$S(t) = -1 + \frac{2}{n+1}\exp\left(-\frac{t}{\tau_D}\right) + \frac{2n}{n+1}\exp\left(-\frac{1+n}{2n} M_2^{IS} t^2\right) \tag{7}$$

The rapid Gaussian decay towards $(1-n)/(n+1)$ is due to the destructive interference of the orientation-dependent coherences while the slower decrease towards -1 characterized by τ_D results from an equilibration of energy within the proton spin system through spin diffusion. For isolated CH_n groups, the CH, CH_2 and CH_3 signals should reach a quasi-equilibrium value equal to 0, $-1/3$ and $-1/2$, respectively. This slight difference in the initial quasi-equilibrium states of cross-polarization has nevertheless been used successfully to discriminate betwen the CH and CH_2 resonances.[23–26]

Density matrix approach

In the case of an S spin with strong dipolar couplings to I spins, CP dynamics in HH-matched spin-lock experiments may be adequately described by the model originally introduced by Müller *et al.*[7] The system is then treated as a tightly coupled CH_n group immersed in a thermal bath consisting of the remaining protons. Neglecting $T_{1\rho}$ relaxation, the reduced density operator σ describing the subsystem evolves under the quantum

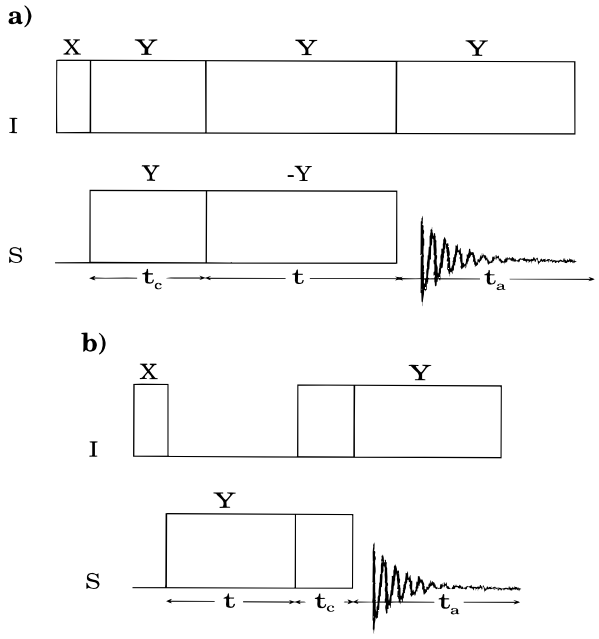

Figure 1. Pulse sequences used. (a) Inversion–recovery cross-polarization (IRCP) experiment; (b) wideline separation (WISE) experiment.

mechanical master equation[7,39]

$$\frac{d}{dt}\sigma(t) = -i[H, \sigma(t)] - \Gamma[\sigma(t) - \sigma(\infty)] \tag{8}$$

In the 'doubly rotating' interaction frame, the Hamiltonian H is given after the usual high-field truncations by[2,39]

$$H = H_I + H_S + H_{IS} + H_{II} \tag{9}$$

where

$$\begin{aligned} H_I &= \omega_{1I} \sum_{k=1}^{n} I_{kx} \\ H_S &= \omega_{1S} S_x \\ H_{IS} &= \sum_{k=1}^{n} 2b_k I_{kz} S_z \\ H_{II} &= \sum_{j>k}^{n} d_{jk}\left[2I_{jz}I_{kz} - \frac{1}{2}(I_j{}^+ I_k{}^- + I_j{}^- I_k{}^+)\right] \end{aligned} \tag{10}$$

where ω_{1I} and ω_{1S} are the radiofrequency (r.f.) field strengths. In MAS experiments, the dipolar couplings b_k and d_{jk} are periodic functions of time. The phenomenological isotropic spin diffusion superoperator which brings the directly bound I spins into thermal equilibrium with the reservoir of the remaining protons with a rate $R = 1/T$ is represented by[7]

$$\begin{aligned} \Gamma(\sigma) = \sum_{k=1}^{n} R\{&[I_{kx}, [I_{kx}, \sigma]] \\ &+ [I_{ky}, [I_{ky}, \sigma]] + [I_{kz}, [I_{kz}, \sigma]]\} \end{aligned} \tag{11}$$

The expression of the S spin magnetization is given by

$$S(t) = Tr[\sigma(t)S_x] \tag{12}$$

As described previously,[14] two different time constants, T_{dp} and T_{df}, may be introduced in Γ so that T_{dp}

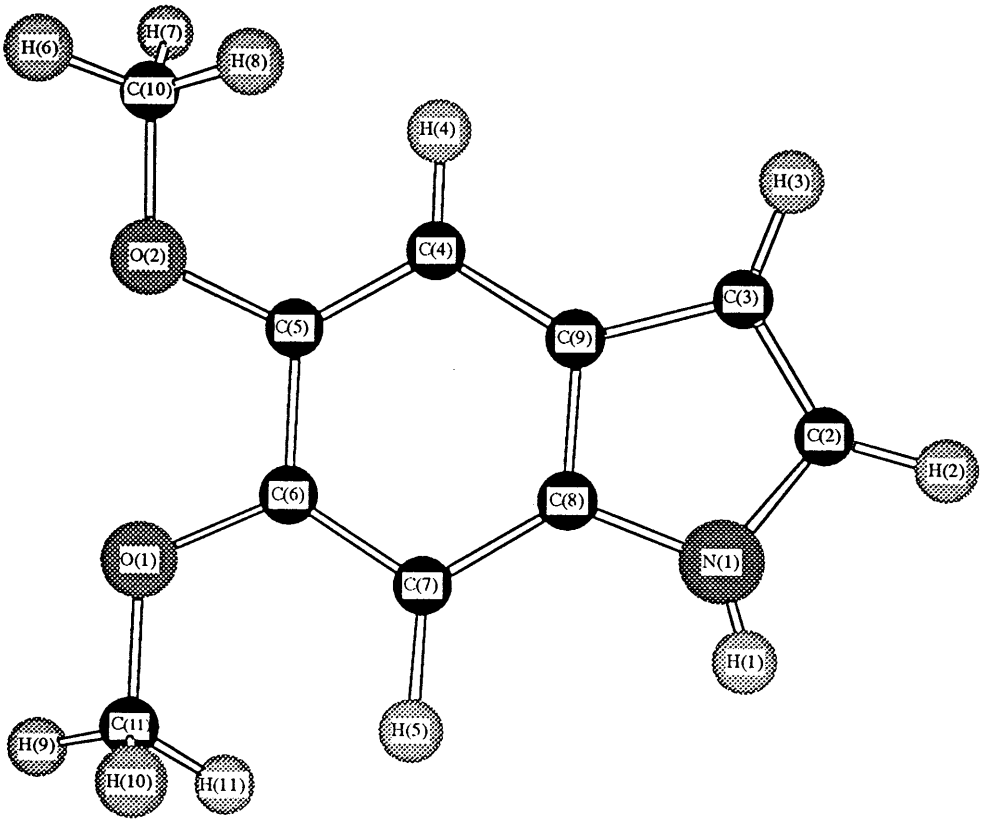

Figure 2. Molecular structure of 5,6-dimethoxyindole (DMI).

only acts on the decay or damping of the coherences while the 'effective spin diffusion process' is completely controlled by T_{df}.

EXPERIMENTAL

The NMR experiments were performed at room temperature on a Bruker MSL-300 spectrometer at a ^{13}C frequency of 75.47 MHz and equipped with a Bruker MAS probe using a cylindrical 7 mm o.d. zirconia rotor. The proton and carbon r.f. fields were carefully adjusted to fulfil the HH condition $|\omega_{1I}|/2\pi = |\omega_{1S}|/2\pi =$ 50 kHz. The pulse sequences shown in Fig. 1 were employed. The preparation period of the IRCP sequence[18,19] consists of a classical cross-polarization period [Fig. 1(a)]. The rare ^{13}C spins are then polarized via HH contact to the abundant ^{1}H spins. This period is followed by a sudden phase reversal, for example, of the carbon r.f. field, inverting the spin temperature of the carbons. Thus, during the evolution time, the carbon magnetization is progressively inversed. During the detection period, the ^{13}C spin magnetization is acquired in the presence of heteronuclear decoupling. In principle, there is no fundamental difference in the spin dynamics between the CP and IRCP experiments. However, IRCP is superior to CP because the signal goes through zero at a definite time (independent of the size of the initial and final polarization) and, thus, better reveals the details of the cross-polarization process. Moreover, in IRCP, the signal-to-noise ratio is enhanced by a factor of two.

Pulse sequences have also been introduced for measuring dipolar local fields from indirect observation of ^{1}H nuclei.[28–33] One of these sequences for wideline separation (WISE) is shown in Fig. 1(b). After the 90° pulse in the proton channel, proton transverse relaxation is permitted to occur during the evolution time t, the heteronuclear dipolar effects being suppressed by a carbon decoupling irradiation. Subsequently, carbon magnetization is created by a short CP mixing time t_c and monitored in the detection period t_a. It should be noted that t_c must be chosen long enough to ensure a sizeable transfer but short enough to depolarize only the immediate vicinity of the S spin. This condition is fulfilled with $t_c \approx 30$–100 μs by CH and CH_2 groups in many organic solids.[34,36] Hence, in principle, the pulse sequence in Fig. 1(b) allows the indirect measurement of the local free induction decay (FID) of protons directly bound to different types of carbons.

The evolution of the reduced density matrix σ was calculated by integrating numerically the master equation [Eqn (8)] using the fourth-order Runge–Kutta method according to Merson[40] (Harwell subroutine DA01A). The evolution of the carbon magnetization $S(t)$ during both the IRCP and WISE experiments were fitted using Powell's method[41] from the numerical recipes package.[42]

A polycrystalline sample of ferrocene was purchased from Fluka. 5,6-Dimethoxyindole (DMI, Fig. 2) was synthesized by A. Lagrange at L'Oréal Research Laboratories, France. Isotactic polypropylene (IPP) was purchased from Brickmann.

RESULTS AND DISCUSSION

Cross-polarization dynamics

Figure 3(a) shows the evolution of the carbon magnetization in the IRCP experiment for a ferrocene powder sample under MAS at a spinning frequency of 4.3 kHz. The two-stage character of the carbon polarization inversion is clearly visible in agreement with previous results.[8,13,14,20] In addition, since the inhomogeneous ^{13}C–^{1}H dipolar interactions are periodically refocused by MAS, strong rotational echoes are apparent at times $t_N = 2N\pi/\omega_r$, $N = 1, 2$, etc. All these features are seen to be very well described by a fit of the experimental data using the memory function approach [Eqn (6)] with $n = 1$ [Fig. 3(a)]. Furthermore, the fact that the spin diffusion time τ_D is close to the dipolar correlation time τ_c demonstrates that the molecules of ferrocene are fairly well isolated from each others, as expected from the crystal structure.[36] Figure 3(b) shows that the CP process is also far from being exponential for the methyl groups of DMI (Fig. 2). To our knowledge, the matched

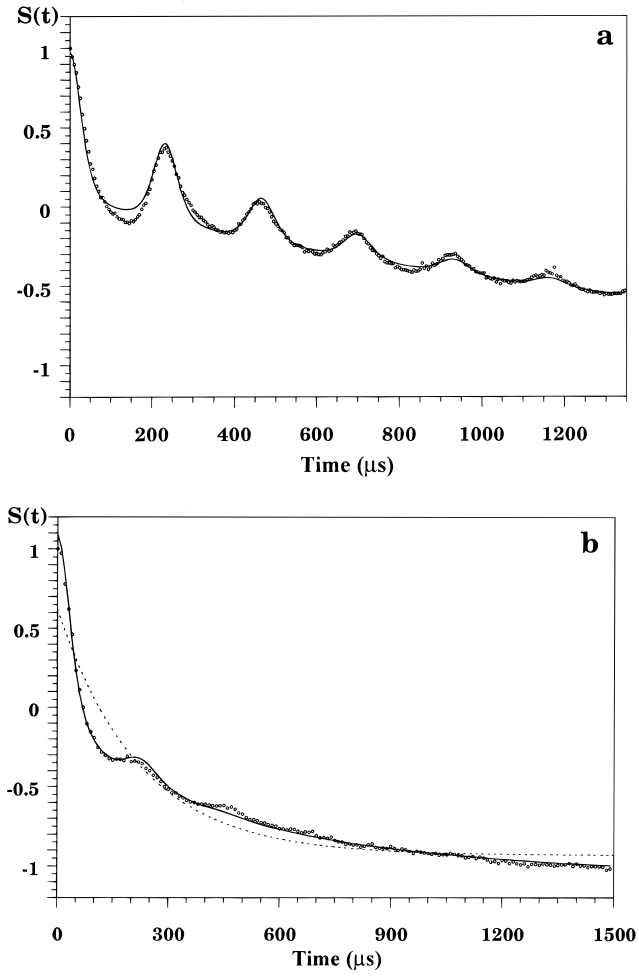

Figure 3. Decay of the carbon magnetization (○) in the IRCP experiment [Fig. 1(a)] for (a) a ferrocene powder sample and (b) the methyl groups of DMI under MAS at $\nu_r = 4.3$ kHz ($t_c = 2$ ms). The solid line represents the fit of the experimental data using the memory function approach [Eqn (6)] with the following parameters: (a) $n = 1$, $1/\sqrt{M_2^{IS}} = 26.3$ μs, $\tau_c = 1.13$ ms, $\tau_D = 1.47$ ms; (b) $n = 3$, $1/\sqrt{M_2^{IS}} = 28.9$ μs, $\tau_c = 180$ μs, $\tau_D = 824$ μs. The broken line represents the exponential fit to the experimental data.

HH cross-polarization process of methyl groups (CH_3) has always been considered to be exponential[26,37] as a result of motional averaging of the heteronuclear interactions, although a two-stage behavior has recently been noticed.[43,44]

As in the case of ferrocene, the memory function approach successfully accounts for the experimental data. Notably, the first rotational echo at t_1 is well described by our fit. Moreover, the short value of τ_c agrees with the expected rapid establishment of a quasi-equilibrium state due to relatively large ^1H–^1H interactions within the CH_3 subsystem. The two-stage feature signifies that the cross-polarization between the CH_3 groups and other protons also belong to the diffusion bottleneck limit, so that the proton spin system cannot be described by a single spin temperature. Note that for both the CH and CH_3 groups in Fig. 3 the condition $\sqrt{M_2^{IS}} \approx \omega_r$ is verified. On the other hand, when $\sqrt{M_2^{IS}} > \omega_r$, careful inspection of Fig. 4 shows that the memory function description does not give a good agreement with the experimental IRCP data for both the CH and CH_2 sites of IPP under MAS at a spinning frequency of 5.5 kHz. Indeed, although the relative amplitude of the fast and slow decays is approximately well described for the CH_2 site, the calculations do not account for the transient oscillations observed in the 50–200 μs range of CP times which arise from coherent energy transfer.[7,8,11–16] Furthermore, note that the amplitude of the rapid coherent decay is underestimated by the model of a C–H pair. Obviously, the absence of transient oscillations comes from the 'Gaussian' form of the memory function model [Eqn (7)].

As expected, this feature is adequately described by the density matrix approach [Eqn (8)] applied to the two-spin CH ($n = 1$) or three-spin CH_2 ($n = 2$) subsystems (Fig. 5). Moreover, the fitted C–H distances $r_{CH} = 1.05$–1.10 Å and H—C—H bond angle ($117 \pm 8°$) are in good agreement with expected values.[13,14,45–47] However, Fig. 5 shows that full agreement with the IRCP experimental data is not obtained for the CH site after the turning point between the two stages, at *ca* 50 μs, the amplitude of the coherent decay being underestimated as with the memory function approach (Fig. 4). This feature, previously attributed to the fact that the C–H pair is not well isolated, has been conveniently taken into account by introducing two time constants, $T_{df}^{(1)}$ and $T_{df}^{(2)}$, into the spin diffusion superoperator Γ.[14] This model leads to two-exponential spin diffusion decays. However, we think that a more physically satisfactory description consists in including explicitly a second proton neighbor into the Hamiltonian H ($n = 2$). Figure 5 shows that this improved model provides excellent agreement with the experimental data in the whole recorded time range. Moreover, the fitted parameters, $r_{CH} = 1.10 \pm 0.02$ Å, T_{dp} and T_{df}, are now found to be identical within experimental accuracy with those obtained for the CH_2 site (Fig. 5). Hence it may be concluded that the consideration of a second proton neighbor located at a distance of *ca* 1.7 Å from the CH carbon site provides a good description of the interactions with the first proton neighbors other than the directly bound proton, the fitted H(1)—C—H(2) angle (86°) being, of course, meaningless. Indeed, the crystal structure of IPP[48] shows the presence of four proton neighbors located at *ca* 2.1 Å from the CH carbon site.

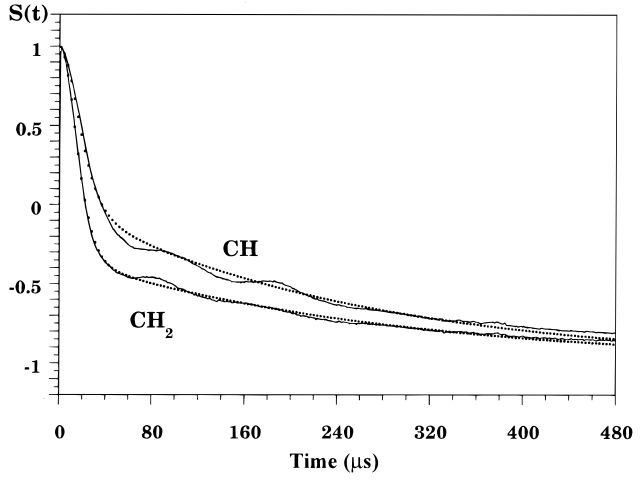

Figure 4. IRCP experimental curves (solid lines) for the CH and CH_2 groups of IPP under MAS at $\nu_r = 5.5$ kHz ($t_c = 2$ ms). The dotted line represents the fit of the experimental data using the memory function approach [Eqn (6)] with the following parameters: (CH) $n = 1$, $1/\sqrt{M_2^{IS}} = 15.4$ μs, $\tau_c = 90$ μs, $\tau_D = 255$ μs; (CH_2) $n = 2$, $1/\sqrt{M_2^{IS}} = 11.6$ μs, $\tau_c = 127$ μs, $\tau_D = 279$ μs.

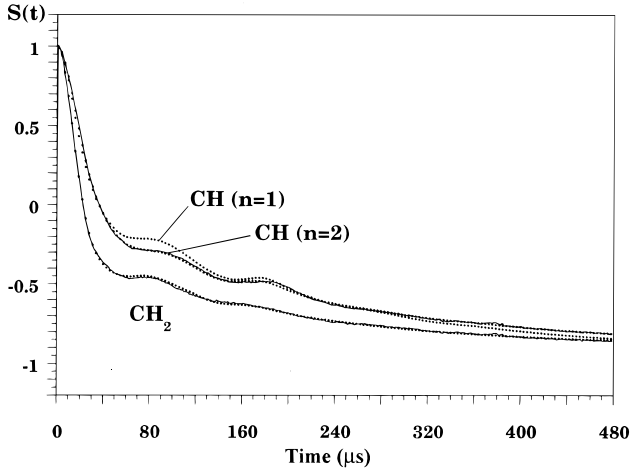

Figure 5. IRCP experimental curves (solid lines) for the CH and CH_2 groups of IPP under MAS at $\nu_r = 5.5$ kHz ($t_c = 2$ ms). The dotted line represents the fit of the experimental data using the density matrix approach with the following parameters: (CH, $n = 1$) $r_{CH} = 1.05 \pm 0.02$ Å, $T_{dp} = 44 \pm 10$ μs, $T_{df} = 174 \pm 20$ μs; (CH, $n = 2$) $r_{CH}(1) = 1.10 \pm 0.02$ Å, $r_{CH}(2) = 1.66 \pm 0.06$ Å, H(1)—C—H(2) angle $= 86 \pm 10°$, $T_{dp} = 60 \pm 10$ μs, $T_{df} = 253 \pm 20$ μs; (CH_2) $r_{CH} = 1.10 \pm 0.02$ Å, H—C—H angle $= 117 \pm 8°$, $T_{dp} = 50 \pm 10$ μs, $T_{df} = 221 \pm 20$ μs.

^1H dipolar local field measurements

In agreement with previous results,[33,34] Fig. 6 demonstrates that the CH and CH_2 groups of IPP can also be readily distinguished using the WISE experiment of Fig. 1(b). Indeed, the CH_2 FID exhibits a strong oscillating behavior corresponding to a tightly coupled ^1H–^1H spin pair, its Fourier transform yielding a Pake-like doublet,[3] while the CH signal is well approximated by a longer and nearly Gaussian decay. Thus, it may be concluded that the WISE experiment offers an alternative approach to the IRCP experiment on performing spectral editing. Indeed, we verified on several organic compounds that it is generally possible to obtain the CH

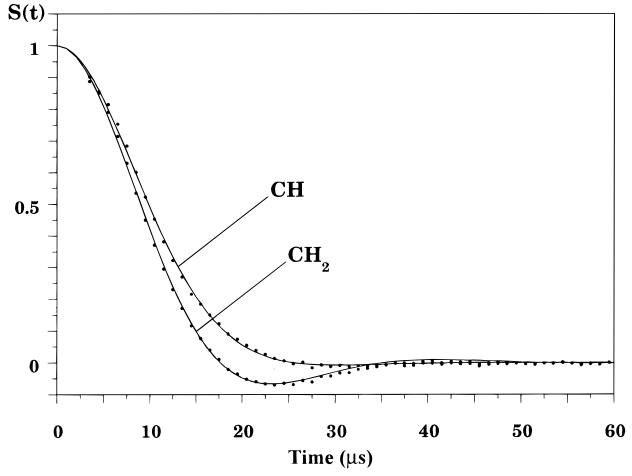

Figure 6. Decay of the carbon magnetization (●) in the WISE experiment [Fig. 1(b)] for the CH and CH_2 groups of IPP under MAS at $\nu_r = 5$ kHz ($t_c = 30$ μs). The solid lines represent the fits of the experimental data using the modified Abragam function [Eqn (13)] with the following parameters: $M_2''(CH) = (1.36 \pm 0.15) \times 10^{10}$ rad^2 s^{-2}; $M_2''(CH_2) = (1.74 \pm 0.15) \times 10^{10}$ rad^2 s^{-2}.

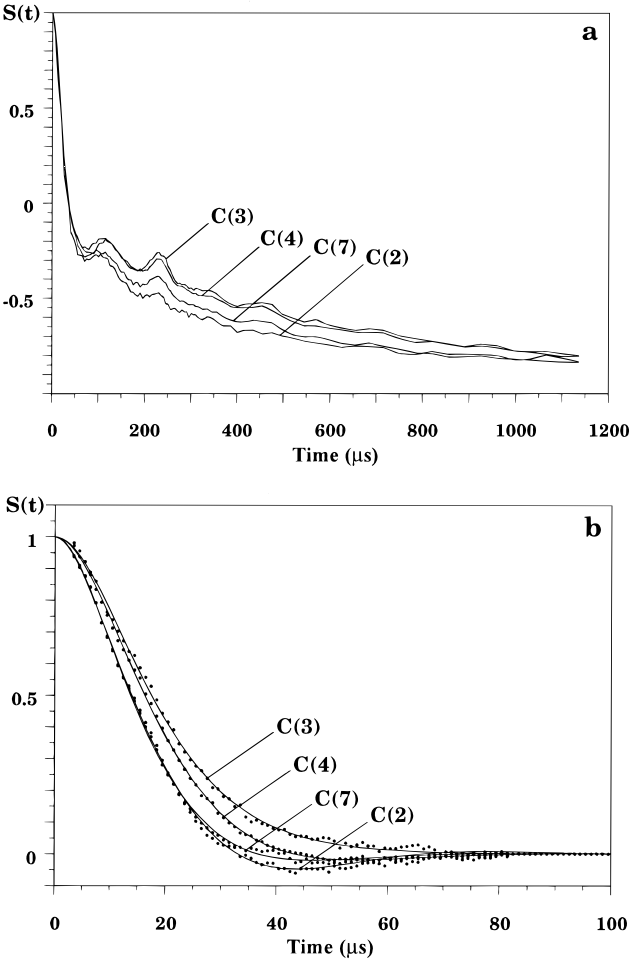

Figure 7. IRCP (a, solid line) and WISE (b, ●) experiments for the different C–H pairs [C(2), C(3), C(4) and C(7)] of DMI under MAS at $\nu_r = 4.3$ kHz. (b) The solid lines represent the fits of the experimental data using the modified Abragam function [Eqn 13] with the following parameters: $M_2''(2) = (1.30 \pm 0.15) \times 10^{10}$ rad^2 s^{-2}; $M_2''(3) = (6.43 \pm 0.60) \times 10^9$ rad^2 s^{-2}; $M_2''(4) = (7.34 \pm 0.70) \times 10^9$ rad^2 s^{-2}; $M_2''(7) = (1.09 \pm 0.10) \times 10^{10}$ rad^2 s^{-2}.

and CH_2 signals with positive and negative intensities, respectively, by setting the evolution time t to *ca.* 18 μs. We checked that the CH_n local FIDs of Fig. 6 are essentially independent of the contact time for t_c in the range 30–50 μs. In order to take into account properly the finite length of the 90° pulse (the origin of the FID is taken at the middle of the 5 μs pulse), an analysis of the signal in the time domain is preferred. In Fig. 6, it is seen that the CH and CH_2 signals of IPP are well fitted by the modified Abragam function[49]

$$S(t) = \exp\{-a^2\tau_S{}^2[\exp(-t/\tau_S{}^2) - 1 - t/\tau_S]\}\,\frac{\sin(bt)}{bt} \tag{13}$$

whose second moment, M_2^{II} is equal to $a^2 + b^2/3$.

Note that, depending on the value of $a\tau_S$, the factor $\exp\{\cdots\}$ of $S(t)$ varies between a Gaussian and an exponential decay with a finite second moment a^2. The resulting experimental values of M_2^{II} for the CH and CH_2 signals are $M_2^{II}(CH) = (1.36 \pm 0.15) \times 10^{10}$ rad^2 s^{-2} and $M_2^{II}(CH_2) = (1.74 \pm 0.15) \times 10^{10}$ rad^2 s^{-2}, while the calculated values of M_2^{II} for each proton site of IPP from the atomic positions of the crystal structure[48] are $M_2^{II}(CH) = 1.21 \times 10^{10}$ rad^2 s^{-2} and $M_2^{II}(CH_2) = 2.80 \times 10^{10}$ rad^2 s^{-2}. Hence, although good agreement between the experimental and calculated M_2^{II} is observed for the CH site, $M_2^{II}(CH_2)$ is found to be much smaller than predicted from the crystallographic data. As expected, this is due to the fact that the positions of the protons are not accurately defined by x-ray diffraction spectroscopy. Indeed, the C—H bond length given by this method is as short as 0.95 Å[48] while the IRCP data yield $r_{CH} = 1.10$ Å (Fig. 5).

When correcting the atomic positions of IPP using the expected C—H internuclear distance $r_{CH} = 1.1$ Å,[13,14] $M_2^{II}(CH_2)$ is drastically reduced to 1.69×10^{10} rad^2 s^{-2} as a consequence of the increase in the H—H distance in the CH_2 group from 1.54 to 1.78 Å. On the other hand, $M_2^{II}(CH)$ stays essentially unaffected by the increase of r_{CH} because in this case there is no dominant dipolar coupling. Hence it is concluded that the second moment of the local FID measured with the WISE experiment is in good agreement with the calculated local M_2^{II} value deduced from the crystal structure of IPP for both the CH and CH_2 sites, although we have neglected any distortion of $S(t)$ due to the orientation dependent cross-polarization process, i.e. a quasi-equilibrium state is assumed to be established after $t_c =$ 30 μs. Note that this assumption is nevertheless in good agreement with the observed short value of $T_{dp} \approx 50$–60 μs (Fig. 5). Moreover, in this analysis we have considered that the ^{13}C magnetization after t_c is due exclusively to the directly bound protons.

The rate of the spin diffusion process accomplished by energy-conserving flip-flop transitions of neighbor spin pairs is known to be related to the strength of the local dipolar field.[36,50,51] In a recent investigation of the local spin diffusion process in DMI,[14] we observed distinct local spin diffusion rates for each non-equivalent proton atoms of this molecule using the ^{13}C-detected proton spin diffusion (SD) experiment developed by Zhang *et al.*[36] This was found to be

entirely consistent with the fact that the different protonated carbon atoms of DMI are clearly distinguished during the second stage of the IRCP experiment [Fig. 7(a)].[14] Since the local fields of protons can be assessed by the WISE experiment of Fig. 1(b), it is of interest to apply to this technique to DMI. Indeed, the results reported in Fig. 7(b) show four distinct local FIDs corresponding to the four different protonated carbon sites of DMI, C(2), C(3), C(4) and C(7) (Fig. 2). As in the case of IPP, it is seen that these local FIDs are well fitted by the modified Abragam function given by Eqn (13). Moreover, the resulting local second moments M_2^{II} are observed to verify the relation $M_2^{II}(2) > M_2^{II}(7) > M_2^{II}(4) > M_2^{II}(3)$. This classification is found to be entirely consistent with the one of the previously measured local spin diffusion time constants T_S:[14] $T_S(3) > T_S(4) > T_S(7) > T_S(2)$. As expected, the same order is obtained during the second stage of the IRCP experiment [Fig. 7(a)]. Furthermore, assuming that T_S is inversely proportional to the square root of the second moment,[6,36,50] the large difference between the local proton spin diffusion decays at the adjacent C(2) and C(3) sites [$T_S(2)/T_S(3) = 0.72$] observed with the SD experiment[14] is remarkably well accounted for by the ratio of the local second moments measured with the WISE experiment, $\sqrt{M_2^{II}(3)/M_2^{II}(2)} = 0.70$. The time constants of the spin diffusion decays in DMI have been previously related to the local intra- and intermolecular network of dipole interactions.[14]

CONCLUSION

Non-exponential behavior has been observed in matched Hartmann–Hahn cross-polarization experiments for all types of CH_n groups ($n = 1$, 2 and 3). The oscillation of the signal implies that under these conditions the spin-temperature concept is invalid. This situation is the common characteristic of evolving systems within the dipolar fluctuation correlation time. In this case, neither the pure quantum-mechanical description nor the pure statistical description can give complete explanation of the evolution of the system. In this paper, we have shown that the experimental data can often be conveniently accounted for by a memory function approach providing a simple physical picture of the cross-polarization dynamics. However, a better description of the spin dynamics requires the use of a density matrix approach. Indeed, when applied to the CH site of isotactic polypropylene (IPP), where fast spin diffusion is present, this method shows that internuclear interactions other than the one with the directly bonded proton must be explicitly considered.

^{13}C-detected measurements of proton dipolar local field are found to be very useful to obtain insight into the local network of dipolar interactions. In IPP, the second moments of the local FIDs are in good agreement with calculated values. Moreover, in DMI, these local FIDs have been related to the local spin diffusion process controlling the second stage of the cross-polarization dynamics. These observations indicating that the local proton environment of the C–H pairs of DMI differ greatly from each other also show that the simple picture of a *common* dipolar fluctuation of protons is not valid. This fact clearly implies that the spin fluctuation spectrum[52] is not uniform over the crystal of DMI.

Acknowledgements

The authors are grateful to the Région Alsace for its participation in the purchase of the Bruker MSL-300 spectrometer and to L'Oréal for financial support. P.R. thanks L'Oréal for a stipend.

REFERENCES

1. A. Pines, M. G. Gibby and J. S. Waugh, *J. Chem. Phys.* **56**, 1776 (1971).
2. M. Mehring, *High Resolution NMR in Solids*. Springer, Berlin (1983).
3. C. A. Fyfe, *Solid State NMR for Chemists*. CFC Press, Guelph (1983).
4. A. Pines, M. G. Gibby and J. S. Waugh, *J. Chem. Phys.* **59**, 569 (1973).
5. D. E. Demco, J. Tegenfeldt and J. S. Waugh, *Phys. Rev. B* **11**, 4133 (1975).
6. T. T. P. Cheung and R. Yaris, *J. Chem. Phys.* **72**, 3604 (1980).
7. L. Müller, A. Kumar, T. Baumann and R. R. Ernst, *Phys. Rev. Lett.* **32**, 1402 (1974).
8. M. H. Levitt, D. Suter and R. R. Ernst, *J. Chem. Phys.* **84**, 4243 (1986).
9. X. Wu, S. Zhang and X. Wu, *Phys. Rev. B* **37**, 9827 (1988).
10. X. Wu, X. Xie and X. Wu, *Chem. Phys. Lett.* **162**, 325 (1989).
11. X. Wu and S. Zhang, *Chem. Phys. Lett.* **156**, 79 (1989).
12. P. Tekely, F. Montigny, D. Canet and J. J. Delpuech, *Chem. Phys. Lett.* **175**, 401 (1990).
13. P. Palmas, P. Tekely and D. Canet, *J. Magn. Reson., Ser. A* **104**, 26 (1993).
14. J. Hirschinger and M. Hervé, *Solid State Nucl. Magn. Reson.* **3**, 121 (1994).
15. G. Hawkes, M. D. Mantle, K. D. Sales, S. Aime, R. Gobetto and C. J. Groombridge, *J. Magn. Reson., Ser. A* **116**, 251 (1995).
16. R. Pratima and K. V. Ramanathan, *J. Magn. Reson., Ser. A* **118**, 7 (1996).
17. S. J. Opella and M. H. Frey, *J. Am. Chem. Soc.* **101**, 5854 (1979).
18. N. Zumbulyadis, *J. Chem. Phys.* **86**, 1162 (1987).
19. D. G. Cory, *Chem. Phys. Lett.* **152**, 431 (1988).
20. X. Wu, S. Zhang and X. Wu, *J. Magn. Reson.* **77**, 343 (1988).
21. X. Wu, S. Zhang and X. Wu, *Chem. Phys. Lett.* **162**, 321 (1989).
22. J. S. Hartmann and J. A. Ripmeester, *Chem. Phys. Lett.* **168**, 219 (1990).
23. X. Wu and K. W. Zilm, *J. Magn. Reson., Ser. A* **102**, 205 (1993).
24. X. Wu and K. W. Zilm, *J. Magn. Reson., Ser. A* **104**, 119 (1993).
25. X. Wu, S. T. Burns and K. W. Zilm, *J. Magn. Reson., Ser. A* **111**, 29 (1994).
26. R. Sangill, N. Rastrup-Andersen, H. Bildsoe, H. J. Jakobsen and N. C. Nielsen, *J. Magn. Reson., Ser. A* **107**, 67 (1994).
27. M. T. Melchior, Poster B-29, presented at the 22nd Experimental NMR Conference, Asilomar (1981).
28. P. Tekely, D. Nicole, J. Brondeau and J. J. Delpuech, *J. Phys. Chem.* **90**, 5608 (1986).
29. N. Zumbulyadis, *Phys. Rev. B* **33**, 6495 (1986).
30. A. J. Vega, *J. Am. Chem. Soc.* **110**, 1049 (1988).
31. P. Tekely, D. Canet and J. J. Delpuech, *Mol. Phys.* **67**, 81 (1989).

32. K. Schmidt-Rohr, J. Clauss and H. W. Spiess, *Macromolecules* **25**, 3273 (1992).
33. P. Tekely, P. Palmas and P. Mutzenhardt, *Macromolecules* **26**, 7363 (1993).
34. P. Palmas, P. Tekely and D. Canet, *Solid State Nucl. Magn. Reson.* **4**, 105 (1995).
35. S. Zhang, B. H. Meier and R. R. Ernst, *Phys. Rev. Lett.* **69**, 2149 (1992).
36. S. Zhang, B. H. Meier and R. R. Ernst, *Solid State Nucl. Magn. Reson.* **1**, 313 (1992).
37. F. Engelke, T. Kind, D. Michel, M. Pruski and B. C. Gerstein, *J. Magn. Reson.* **95**, 286 (1991).
38. P. W. Anderson and P. R. Weiss, *Rev. Mod. Phys.* **25**, 269 (1953).
39. R. R. Ernst, G. Bodenhausen and A. Wokaun, *Principles of Nuclear Magnetic Resonance in One and Two Dimensions*. Oxford University Press, Oxford (1987).
40. R. H. Merson, in *Proceedings of a Symposium on Data Processing*. W. R. E., South Australia (1947).
41. M. J. D. Powell, *Comput. J.* **7**, 303 (1965).
42. W. H. Press, B. P. Flannery, S. A. Teukolsky and W. T. Fetterling, *Numerical Recipes*. Cambridge University Press, Cambridge (1986).
43. S. Ding, C. A. McDowell and C. Ye, *J. Magn. Reson., Ser. A* **109**, 1 (1994).
44. S. Ding, C. A. McDowell and C. Ye, *J. Magn. Reson., Ser. A* **109**, 6 (1994).
45. R. K. Hester, J. L. Ackerman, V. R. Cross and J. S. Waugh, *Phys. Rev. Lett.* **34**, 993 (1975).
46. E. F. Rybaczewski, B. L. Neff, J. S. Waugh and J. S. Sherfinski, *J. Chem. Phys.* **67**, 1231 (1977).
47. T. Nakai and T. Terao, *Magn. Reson. Chem.* **30**, 42 (1992).
48. A. Immirzi and P. Iannelli, *Macromolecules* **21**, 768 (1988).
49. A. Abragam, *The Principles of Nuclear Magnetism*. Oxford University Press, Oxford (1961).
50. T. T. P. Cheung, *Phys. Rev. B* **23**, 1404 (1981).
51. D. Suter and R. R. Ernst, *Phys. Rev. B* **32**, 5608 (1985).
52. D. A. McArthur, E. L. Hahn and R. E. Walstedt, *Phys. Rev.* **188**, 609 (1969).

